Numerical Study on Effect of Projectile Shape Change by Ablation in RAMAC30

Kunmin Sung[1], In-seuck Jeung[1]
Friedrich Seiler[2], Gunther Patz[2], Günter Smeets[2] and Julio Srulijes[2]

[1]Institute of Advanced Aerospace Technology, School of Mechanical and Aerospace Engineering
Seoul National University, 151-742, Seoul, Republic of Korea

[2]French-German Research Institute of Saint-Louis(ISL)
Shock Tube Department

1. Introduction

The concept of ram accelerator is that projectile is flying with synchronized combustion in tube filled with pre-mixed combustible gas mixture. Ram Accelerator facilities have major benefits for hypersonic research. The gas dynamics phenomena in ram accelerator are very similar to those expected ones in scramjet and oblique detonation wave engines. Therefore, study on ram accelerator operation will enhance the understanding of supersonic combustion and hypersonic propulsion system.

Despite the number of research programs around the world, a maximum speed of 2.7 km/s was only available at the UW (University of Washington) ram accelerator facility starting with subsonic combustion behind the projectile which was moving initially at subdetonative speeds [1]. Thus, to obtain higher velocities than 2.7 km/s, combustion mode must be the superdetonative mode, where ignition and combustion occur at supersonic flow speeds in the space formed between projectile and tube wall.

Based on this motivation, ISL (French-German Research Institute of Saint-Louis) has developed a rail tube version of a ram accelerator facility named RAMAC 30 version II that directly launched superdetonative speed. In this facility, a cylindrical projectile having conical fore- and after-bodies was launched by a powder gun and accelerated in a ram accelerator tube having four or five guide rails [2]. Although the initial launching speed of a powder gun was only about 1.8 km/s, the superdetonative launch was possible by using the $H_2/O_2/CO_2$ mixture having a lower C-J (Chapman-Jouguet) detonation wave speed than the launching speed.

In the previous experiments, ISL's RAMAC 30 demonstrated that ignition and acceleration was successful with an aluminium projectile but acceleration was not observed in the case of a steel projectile. After the experiment, the aluminium projectile showed ablation with significant mass loss [3]. These facts imply that there is an important ignition mechanism which is strongly related to the melting and combustion of aluminium projectile by friction, and heat conduction.

At the earlier stage of ram accelerator studies, the superdetonative mode operation had been considered to be sustained by an oblique detonation wave in the combustor. Computational studies by Yungster and Bruckner[4] and Li et al.[5] using inviscid flow model and chemical kinetics showed that ram acceleration was possible through this concept at very high velocity ranges. However, more recent viscous analyses by Yungster[6] and Choi et al.[7] showed that combustion could be initiated in the boundary layer due to the aerodynamic heating associated with shock wave / boundary layer interaction at intermediate velocity ranges where shock-heating was insufficient for mixture ignition.

The ISL's ram accelerator experiments, however, revealed that the previous studies on superdetonative combustion characteristics were not applicable to the experimental case and the other combustion characteristics

Correspondence to : enjis@snu.ac.kr

might be more important for the low speed superdetonative mode of operation. Therefore, to understand the combustion mechanism, numerical simulations was conducted for ISL's RAMAC 30 experiments using the experimental configuration and conditions in this study.

2. ISL's RAMAC 30 II Test Facility

Based on the needs of hypersonic launching facility, ISL built two ram accelerators: a 30-mm-caliber-tube, called RAMAC 30, and 90-mm-one, RAMAC 90. The superdetonative combustion mode has been mainly tested in RAMAC 30 which was implemented with rail tube version II since 1997. Figure 1 shows the schematics of RAMAC 30 test facility, which consisted of a pre-accelerator tube, a ram tube containing a combustible gas mixture with both ends sealed by diaphragms which were hit and destroyed by the moving projectile forebody nose tip, and a decelerator tube. Two tubes with a length of 2.4m each were used forming a total ram tube length of 4.8m. Projectiles had an inner magnesium core which was fully covered by an aluminum (or sometimes steel was used for different experimental shots) in the combustor as well as at the fore- and afterbodies. Cylindrical projectiles of 130g~150g, 3.0 cm caliber, and 16.1 cm long, could be accelerated to 1800 m/s at the exit of the pre-accelerator tube before penetrating through the mixture in the rail tube version II.

3. Numerical Methods

For computational study of ram accelerator, a fully coupled form of multi-species conservation equations and Reynolds averaged Navier-Stokes equations coupled with Baldwin-Lomax turbulence modeling was used for axisymmetric geometry. Typical operational pressure of ram accelerator is higher than 50atm and reduced kinetic mechanism for low pressure can not applicable. Therefore finite-rate chemistry model of high pressure should be considered. Petersen and Hanson [8] developed reduced mechanisms to model the combustion characteristics of typical ram accelerator mixtures at pressures approaching 300atm based on the GRI-Mech. In this study, fully detailed 10 species (H, H_2, O, O_2, OH, H_2O, HO_2, H_2O_2, CO, CO_2) and 29 step reaction model for reaction of $H_2/O_2/CO_2$ mixture was considered. Govern equation is discretized by finite volume cell vertex approach. Viscous flux is discretized by central differencing and convective flux is obtained by Roe's flux difference splitting method [9]. Primitive variables are extrapolated at cell interface by MUSCL (Monotonic Upstream method for Scalar Conservation Law) scheme [10]. Discretized equation is time integrated by LU-SGS scheme [11].

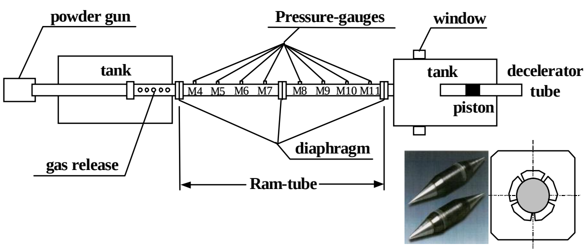

Fig. 1 Schematic of ISL's RAMAC30

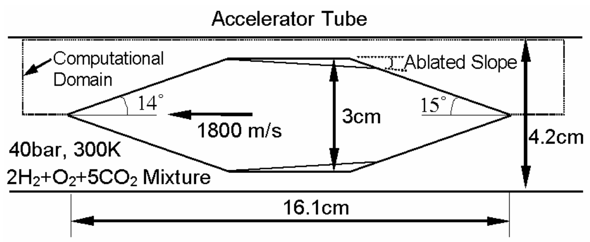

Fig.2 Computational domain

4. Computational Modeling

Figure 2 shows computational conditions and domain. Diameters of a projectile and a tube are 3.0 cm and 4.2 cm, respectively. For the experiment, the tube wall had a decagonal cross-section with five rails but in this study assumed circular for the axisymmetric simulations. Initial launching speed was 1800m/s from the experiment. Acceleration of projectile is computed with area integration of pressure and speed is updated by every step.

Mixtures for shot 225 had a pressure and temperature of 40 bar and 300K, respectively. The gas composition used for shot 225 was $2H_2+O_2+5CO_2$: a stoichiometric H_2/O_2 mixture diluted with 5 moles of CO_2.

The computational domain for the simulation was extended by 1cm before and after the projectile, and it was covered by the 380x100 computational grids that was uniformly distributed in the axial direction and clustered to both walls in the radial direction. Since these simulations had to cover overall flow features of the scale of the entire projectile, the computational resolutions used were limited. Therefore, details of the detonation structure, such as the induction region, might not be well resolved. But our purpose was exploring the overall development and so, current grid resolution was enough to represent the shock and detonation position because the local transit time was sufficiently smaller than the induction time of $2H_2+O_2+5CO_2$ mixture behind the reflected shock where mixture ignition occurred. To investigate effect of shape change by ablation, numerical simulations were conducted for the projectile without ablation and two cases of ablated slope 1° /1.5°. These three simulations have same condition except for slope angle of combustor.

5. Result and Analysis

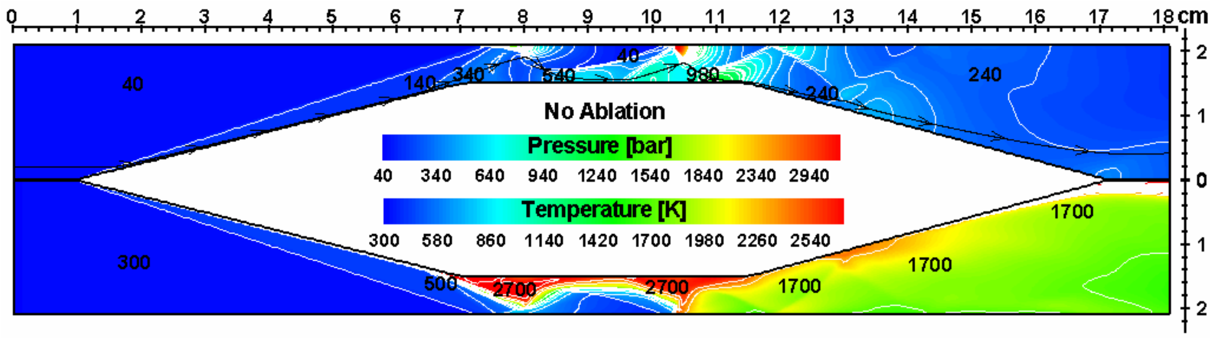

Fig. 3 Pressure and temperature contour at position 20cm (projectile without ablation)

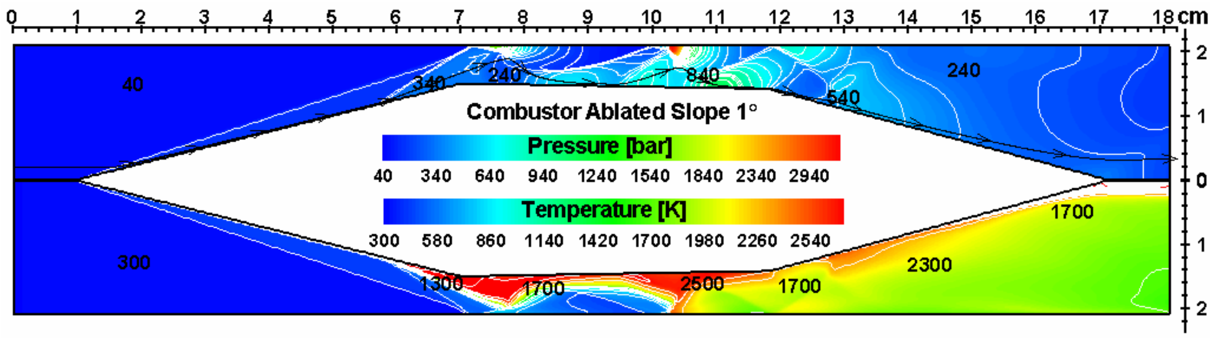

Fig. 4 Pressure and temperature contour at position 20cm (combustor ablated slope 1°)

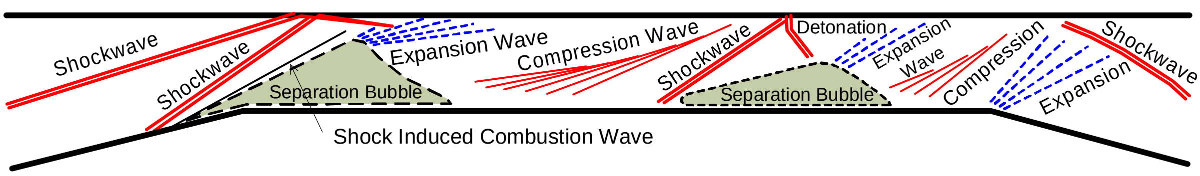

Fig. 5 Schematics of Shockwave and Flame Structure

Figure 3 and 4 show pressure and temperature contour for the case of projectile without ablated and with ablated slope 1° respectively. Overall structure of shockwaves are almost same, shockwave is relatively stiff in the case of no ablation. Streamline in pressure contour show two separation bubbles in combustor region, first one is at entrance of combustor and another one is at rear part of combustor. In temperature contour, there are high temperature region in two separation bubble and behind detonation wave. Figure 5 shows schematics of shockwave and flame structure. Incidence shockwave generated by first separation bubble is combined with shockwave induced by fore-cone at tube wall. There is shock-induced combustion wave behind incident shockwave but very small amount of mixture is passing through this wave. Expansion wave and recompression structure appear behind first bubble. Second separation bubble also makes induced shockwave and this shock reflected at tube wall. Mixture is heated enough for reaction by compression wave/induced shockwave. Also mixture is pressurized by shockwave/ reflected shockwave. There is strong detonation wave very behind reflected shockwave. Most mixture reacts and release heat at this detonation wave. There is also expansion wave and compression wave structure behind second separation bubble. Exhaust gas expand at nozzle.

Two separation bubbles determine shockwave structure, especially second separation bubble has import role for sustain detonation wave. Without second bubble, flow is not heated enough to initiate reaction and pressure is not high enough to sustain detonation wave. In the other point of view, second separation bubble is also sustained by detonation wave. Rotating momentum of separation bubble is supplied by high pressure region behind detonation wave. This interaction between detonation wave and separation bubble makes oscillation of flame structure.

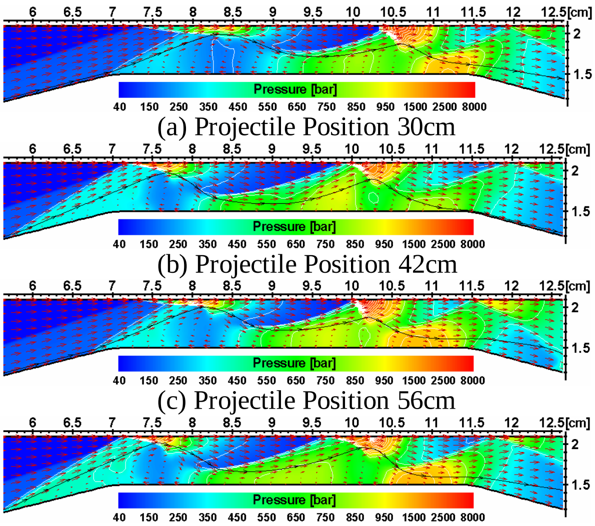

(a) Projectile Position 30cm
(b) Projectile Position 42cm
(c) Projectile Position 56cm
(d) Projectile Position 65cm

Fig. 5 Oscillation of Flame (Without ablation)

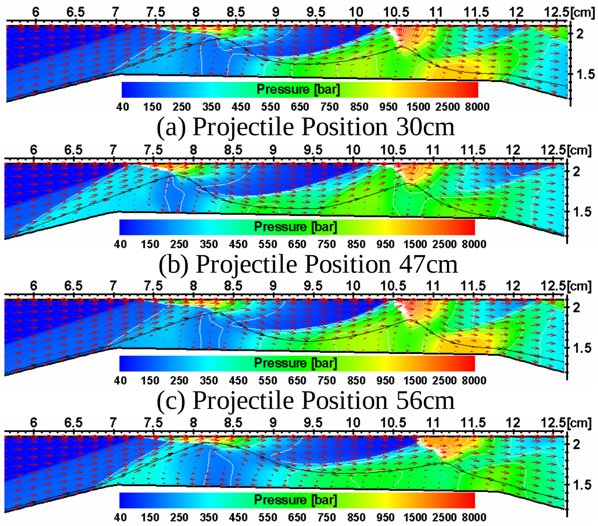

(a) Projectile Position 30cm
(b) Projectile Position 47cm
(c) Projectile Position 56cm
(d) Projectile Position 65cm

Fig. 6 Oscillation of Flame (Combustor ablation slope 1°)

Figure 5 and 6 are shows sequence of flame oscillation for the case of projectile without ablation and with ablated slope 1° respectively. If pressure behind detonation is high enough to sustain separation bubble, separation bubble is more grow and second bubble advance to ahead. Induced shockwave is become more strong make more strong detonation wave. By this mechanism, second separation bubble is grower and grows. Second separation bubble combines with first separation bubble (Figure 5(a) and 6(a)). Second separation bubble supply pressure to first one, first one grows and advances outside of combustor (Figure 5(b) and 6(b)). By advancing of separation bubble, expansion wave behind bubble become stronger and two separation bubbles are disconnected. Consequently, compression wave behind first bubble becomes stronger. First separation bubble is pushed into combustor by momentum of free stream. If pressure behind second separation bubble is still high enough, this sequence repeated (Figure 5(c), 5(d)). But if pressure is not enough, separation bubble becomes weak (Figure 6(c)) and induced shockwave also become weak. By result, detonation wave decay down and run out of combustor (Figure 6(d)).

This oscillation sequence is also holding detonation mechanism which summarized mechanical chocking by detonation wave / separation bubble interaction. If there is ablation, shape of combustor section is changed and have expansion angle. Pressure in combustor decreases relatively and area blocking ration by separation bubble is relatively decrease. Therefore flow choking is not enough for large ablation. In the case of projectile with ablation slope 1.5°, initial structure of flame is almost same another two cases but flame holding mechanism doesn't work properly due to large expansion in combustor section.

Figure 7 shows speed of projectile versus position of projectile. Initial speeds are well matched to experimental result for all cases. For the case of projectile without ablation, increasing rate of speed decay down after 40 cm and speed is slowly increasing to 1840m/sec. For the case of ablation slope 1°, increasing rate of speed decay down after 47cm, speed profile is very well matched to experiment before 47cm. And increasing rate is still well matched until 80cm. In case of ablation angle slope 1.5°, initial speed is highest and increasing rate of speed is higher than one of experiment. But this increasing rate is not continued after 45 cm.

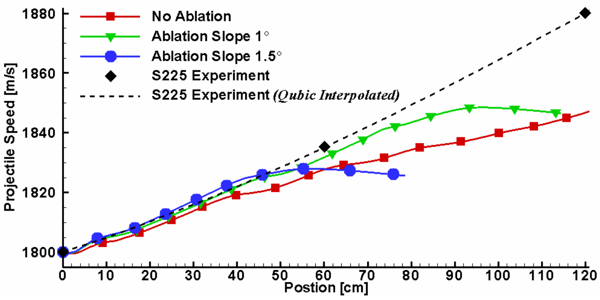

Fig. 7 Speed of projectile

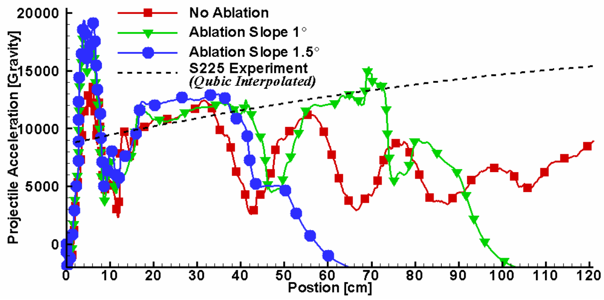

Fig. 8 Acceleration of projectile

Figure 8 shows acceleration of projectile versus position of projectile. Initial overshoot and undershoot of acceleration is due to forced ignition. But these over/undershoot affect during short initial period and averaged initial acceleration is almost equal to experimental result. In the case of projectile without ablation, acceleration fluctuate after 30cm and this is due oscillation of flame. Local minimum of acceleration is at 42cm (Figure 5(b)). Because pressure of first separation bubble is relative high, advancing of separation bubble make pressure drag in fore-body cone. By oscillation of flame, acceleration fluctuating and averaged increment of speed is severely decreased. In case of ablation slope 1°, initial behavior of acceleration between 20cm and 40cm is very well matched. Acceleration decrease by oscillation of flame, but it is weaker than former one. There is maximum acceleration at 71cm and acceleration decreases by extinction of flame. In case of ablation slope 1.5°, has most high initial acceleration but acceleration decrease after 36cm and decelerated by extinction of flame.

6. Conclusion

Shockwave structure is determined by two separation bubbles. Interaction between second separation bubble and detonation wave is key of flame holding mechanism and oscillation of flame. Average acceleration is reduced by oscillation of flame. Shape change by ablation makes expansion in combustor section. This reduces flame oscillation, combustor can produce extra thrust because combustor has normal component along axial direction. Shape change can prevent unstart by strong flame with high pressure. This effect makes ram accelerator more stable and having higher acceleration. For S225 experiment, flame may be stronger with aluminum combustion, but it was not unstart by shape change and had high average acceleration. But shape change also has effect of disturbing mechanism for holding flame. If there is large shape change by severe ablation, it can cause flame out in ram accelerator. Ablation of projectile has both side of aluminum combustion and shape change. Shape change is also important point for understanding operation of ISL's ram accelerator.

Acknowledgement

This work was supported by the Korea Science and Engineering Foundation (KOSEF) through the National Research Lab. Program funded by the Ministry of Science and Technology (No. M10500000072-06J0000-07210) and FVRC(Flight Vehicle Research Center), Seoul National University.

References

[1] Elvander, J.E., Knowlen, C., and Bruckner, A. P. (1988). Ram Accelerators. Springer-Verlag. pp 55-64

[2] Seiler, F., Patz, G., Smeets, G., and Srulijes, J. (1995). Second International Workshop on Ram Accelerators. Seattle, WA, 1995.

[3] Seiler, F., Patz, G., Smeets, G., and Srulijes, J. (1998). AIAA Paper 98-3445, Cleveland, OH.

[4] Yungster, S., and Bruckner, A. P. (1992). Journal of Propulsion and Power, Vol. 8, No. 2, pp 457-463

[5] Li, C., Kailasanath, K., and Oran, E. S. (1997). Combustion and Flame, Vol. 108, pp 173-186

[6] Yungster, S. (1992). AIAA Journal, Vol. 30, No. 10, pp 2379-2387

[7] Choi, J.-Y., Jeung, I.-S., and Yoon, Y. (1998). AIAA Journal, Vol. 36, No. 6, pp 1029-1038

[8] Petersen, E.L. and Hanson, R.K. (1999). Journal of Propulsion and Power, Vol. 15, No. 4, pp 591-600

[9] Roe, P. L. (1981). Journal of Computational Physics, Vol. 43, pp 357-372

[10] Hirsch, C. (1990). Numerical Computation of Internal and External Flows, Vol. 2, John Wiley & Sons, New York

[11] Shuen, S. and Yoon, S. (1989). AIAA Journal, Vol. 27, No. 12, pp. 1752-1760